*The FASEB Journal* express article10.1096/fj.02-0870fje. Published online August 1, 2003.

# Ser-256 phosphorylation dynamics of aquaporin 2 during maturation from the endoplasmic reticulum to the vesicular compartment in renal cells

Giuseppe Procino,* Monica Carmosino,* Oriano Marin,[†] Anna M. Brunanti,[†] Antonella Contri,[†] Lorenzo A. Pinna,[†] Roberta Mannucci,[‡] Soren Nielsen,[§] Tae-Hwan Kwon,[¶] Maria Svelto,*[,#] and Giovanna Valenti*[,#]

*Dipartimento di Fisiologia Generale ed Ambientale, University of Bari, 70126 Bari, Italy; [†]Dipartimento di Chimica Biologica, University of Padova, 35121 Padova, Italy; [‡]Dipartimento di Medicina Clinica e Sperimentale, Universita' di Perugia, 06100 Perugia, Italy; [§]Department of Cell Biology, Institute of Anatomy, University of Aarhus, 8000 Aarhus, Denmark; [¶]Department of Physiology, School of Medicine, Dongguk University, Kyungju 780-714, Korea; [#]Centro di Eccellenza di Genomica Comparata, University of Bari, Italy

Corresponding author: Giovanna Valenti, Dipartimento di Fisiologia Generale ed Ambientale, Via Amendola 165/A, 70126 Bari, Italy. E-mail: g.valenti@biologia.uniba.it

## ABSTRACT

Aquaporin 2 (AQP2) phosphorylation at Ser-256 by protein kinase A (PKA) is a key signal for vasopressin-stimulated AQP2 insertion into the plasma membrane in renal cells. This study underscores the possible role of phosphorylation at Ser-256 in regulating AQP2 maturation. AQP2-transfected renal CD8 cells were incubated with brefeldin A (BFA) to accumulate newly synthesized AQP2 in the endoplasmic reticulum (ER), and AQP2 flow from ER to the vesicular compartment was analyzed after BFA washout. We found that a) in the ER, AQP2 is weakly phosphorylated; b) the amount of phosphorylated AQP2 (p-AQP2) at Ser-256 increased significantly during transit in the Golgi, even in the presence of the PKA inhibitor H89; and c) AQP2 transport from the Golgi to the vasopressin-regulated vesicular compartment occurred with a concomitant decrease in p-AQP2 at Ser-256. These results support the hypothesis that AQP2 transition in the Golgi apparatus is associated with a PKA-independent increase in AQP2 phosphorylation at Ser-256. Conversely, impaired constitutive phosphorylation in a Golgi-associated compartment occurring in cells expressing mutated S256A-AQP2 or E258K-AQP2 causes phosphorylation-defective AQP2 routing to lysosomes. This result might explain the molecular basis of the dominant form of nephrogenic diabetes insipidus caused by the mutation E258K-AQP2, in which the phenotype is caused by an impaired routing of AQP2.

Key words: Golgi casein kinase • PKA • NDI • phosphorylation

The antidiuretic hormone vasopressin (AVP) regulates water reabsorption by the kidney collecting duct through insertion and removal of the aquaporin 2 (AQP2) water channel from the apical membrane of principal cells via a specialized pool of vesicles. AVP-induced phosphorylation of AQP2 at Ser-256 by protein kinase A (PKA) is considered a key signal for its translocation to the apical plasma membrane (1–4). However, a considerable

amount of phosphorylated AQP2 is detected in intracellular vesicles in nonstimulated cells, indicating that AQP2 is, at least in part, constitutively phosphorylated (3–5). Previous studies proposed that a small change in the stoichiometry of phosphorylated and nonphosphorylated monomers in a tetramer might be critical for AQP2 localization, explaining the presence of phosphorylated AQP2 in intracellular vesicles (5). Whereas significant progress has been made in recent years on the requirement for AQP2 phosphorylation at Ser-256 for apical targeting, little is known regarding a putative role of AQP2 phosphorylation in regulating its intracellular trafficking.

Several studies have shown that protein kinases and phosphatases control the sorting within the trans-Golgi network (TGN)/endosomal system (6–8). In particular, the cytoplasmic domains of transmembrane proteins contain sorting signals, including phosphorylation of target aminoacids, that drive segregation of proteins into transport intermediates. PKA and protein kinase C (PKC) activities are also of fundamental importance for the polarized transport of vesicles containing newly synthesized proteins from the TGN to the cell surface (9, 10). Association of PKA and phosphatase activities with AQP2-containing vesicles has been demonstrated (11, 12), suggesting that in situ phosphorylation-dephosphorylation processes are involved in specialized sorting of AQP2-containing vesicles. This study was undertaken to gain a better understanding of the regulatory role of AQP2 phosphorylation dynamics during its maturation from the endoplasmic reticulum (ER) to the vasopressin-regulated vesicular compartment in AQP2-transfected renal CD8 cells. The picture that emerged indicates that phosphorylation of AQP2 at Ser-256 by two distinct kinases, sharing a different subcellular compartmentalization, might be a key signal regulating both AQP2 exit from the Golgi complex and translocation to the plasma membrane.

## MATERIALS AND METHODS

### Cell culture

CD8 cells were established by stably transfecting the RC.SV3 rabbit cortical collecting duct cells (25) with cDNA encoding rat AQP2 (13). CD8 cells were grown at 37°C as described in a hormonally defined medium containing 5% of newborn calf serum. Confluent monolayers were used at days 3–5 after plating.

### DNA constructs and transfection

From pT7Ts-E258K-AQP2 and pT7Ts-S256A-AQP2 (23), 820 bp cDNA fragments, encoding the full-length proteins, were excised using BglII and SpeI. The E258K-AQP2 cDNA fragment was ligated into the BamHI and XbaI sites of pCDNA3 (Invitrogen, Carlsbad, CA), resulting in pCDNA3-E258K-AQP2, whereas the S256A-AQP2 cDNA fragment was ligated into BglII and XbaI sites of the mammalian expression vector pCB6, resulting in pCB6-S256A-AQP2. Both expression constructs contain a Geneticin resistance cassette. Both constructs were made and kindly provided by E.J. Kamsteeg, P. Savelkoul, and P.M.T. Deen (University of Nijmegen, The Netherlands). Transfection of RC.SV3 rabbit cortical collecting duct cells was performed by use of lipofectin reagent (Gibco-BRL, Grand Island, NY) as described previously (13).

**Immunolocalization experiments**

Immunolocalization of AQP2 and p-AQP2 (Ser-256) was performed as previously described (12). Experimental conditions included basal condition, 16 h treatment with 1 μg/ml BFA, BFA treatment followed by 2 h washout in the presence or in the absence of 30 μM H89, BFA treatment followed by 4 h washout. Golgi apparatus was visualized with the fluorescent lipid NBD $C_6$-ceramide complexed to bovine serum albumin (BSA) (Molecular Probes, Eugene, OR). For this purpose, cells grown on coverslips were treated under the conditions indicated, fixed in 4% paraformaldehyde in PBS, stained with NBD $C_6$-ceramide following the manufacturer's instructions, and examined by fluorescence microscopy.

The coverslips were examined with a Leica microscope equipped for epifluorescence. Digital images were obtained using a cooled CCD camera (Princeton Instruments, Monmouth Junction, NJ). In colocalization experiments, cells were double labeled with AQP2 antibody and AC17 anti-Lamp1 monoclonal antibody diluted 1:1000 (26) and revealed with anti-rabbit IgG Alexa Fluor 488 and anti-mouse IgG Alexa Fluor 568 (Molecular Probes), respectively (1:1000 dilution). To test the effect of forskolin ($10^{-4}$ M, 15 min, 37°C) on AQP2 localization, wild-type E258K-AQP2 and S256A-AQP2 mutant cells were labeled with AQP2 antibody and processed as described above. Coverslips were examined by laser scanning confocal microscopy (MRC-1024, Bio-Rad, Hercules, CA) equipped with a krypton/argon mixed gas laser. A specific software for acquisition and processing of confocal images (LaserSharp MRC 1024) was used for image analysis as described previously (12).

When applicable, the extent of colocalization was obtained with the "colocalization" module of Imaris software running on SGI Octane workstation. With this software, white color corresponds to the individual picture localization where the signal of each channel (red and green) falls inside a certain intensity range simultaneously.

**Phosphorylation of AQP2 in intact cells**

Metabolic labeling of confluent monolayers of wild-type E258K-AQP2 and S256A-AQP2 mutant transfected cells with [$^{32}$P] orthophosphoric acid (NEN) was performed as described previously (12). To test the effect of forskolin (FK) on AQP2 phosphorylation, we stimulated wt-AQP2, E258K-AQP2, and S256A-AQP2 expressing cells with FK $10^{-4}$ M for 15 min in the culture medium. In the set of experiments using BFA (Sigma, St. Louis, MO), conditions included basal condition, 16-h treatment with 1 μg/ml BFA, BFA treatment followed by 2-h washout in the presence or in the absence of 30 μM H89, and BFA treatment followed by 4-h washout.

Cells were solubilized for 1 h in ice-cold incubation buffer for immunoprecipitation (150 mM NaCl, 20 mM TRIS, 1 mM EDTA, 1 mM $MgCl_2$, 1 mM $CaCl_2$, 2% Triton X-100, 0.5% Nonidet P40, PMSF 1 mM, pH 7.4), and AQP2 was immunoprecipitated as previously described (12). Immunocomplexes were mixed with 30 μl of Laemmli buffer, heated at 60°C for 15 min, and resolved in a 13% polyacrylamide slab gel. Gels were stained, dried, and exposed to Kodak X-Omat AR film, using a Lightning Plus intensifying screens at –80°C.

To block newly synthesized proteins in the Golgi apparatus, in some experimental conditions, cells were kept at 20°C for 2 h in the culture medium. Experimental conditions for CD8 cells included basal condition (Ctr), 2 h at 20°C (20°C) and 2 h at 20°C followed by 10 min at 37°C (37°C rev). Cells were then lysed and subjected to AQP2 immunoprecipitation as described above.

**Pulse-chase experiments**

CD8 cells were plated in 60-mm culture dishes 1 day before labeling and grown to 70% confluence. Cells were starved of methionine and cysteine by incubation in 4 ml of serum-free Dulbecco's modified Eagle's medium (DMEM) without methionine and cysteine (DMEM$^-$) for 1 h. Pulse-labeling (1 h at 37°C) was carried out by addition of 150 μCi/ml of [$^{35}$S] methionine/cysteine (Redivue PRO-MIX; Amersham Biosciences, Piscataway, NJ) in the same medium. Cells were then washed in complete medium supplemented with 5 mM of L-methionine and 5 mM of L-cysteine and chased in this medium for 0, 4, 8, and 16 h. Where indicated, BFA (1 μg/ml) was added during the chase time. After 16 h of BFA treatment, the drug was washed after 2 or 4 h. Cells were lysed, and AQP2 was immunoprecipitated as described above. Immunocomplexes were mixed with 30 μl of Laemmli buffer, heated at 60°C for 15 min, and resolved in a 13% polyacrylamide slab gel. Gels were stained, dried, and visualized by fluorography, using a PhosphorImager (Storm 820; Molecular Dynamics, Sunnyvale, CA) with ImageQuant software.

**Immunoblotting**

Immunocomplexes were resolved in a 13% polyacrylamide gel, and proteins were electrotransferred to Immobilon-P (Millipore, Bedford, MA) by standard procedures. Immunoblotting was performed as described previously (12, 13). Blots were probed with affinity-purified AQP2 or p-AQP2 antibodies, incubated with goat anti rabbit IgG alkaline-phosphatase conjugated (1:5000; Sigma), and revealed with 1-Step NBT/BCIP (Pierce, Rockford, IL)

**Protein kinases**

Golgi apparatus casein kinase (G-CK) was isolated from the Golgi fraction of rat lactating mammary gland (22) and purified so that it was free of other contaminating kinase activities, as judged by gel-phosphorylation experiments described previously (40). The preparation was free of contaminations from protein kinases other than G-CK as judged from its inability to phosphorylate broad specificity phosphoacceptor substrates such as histones, myelin basic protein (MBP), and poly(E,Y)4:1 and by the observation that its activity on casein is totally unaffected by up to 50 μM staurosporine, a broad specific inhibitor of protein kinases generally effective in the nanomolar range (41, 22). Contamination by "casein kinases" 1 and 2, moreover, was ruled out using sensitive assays with specific peptide substrates of these kinases (21). PKA catalytic subunit was purchased from Biolabs, (Beverly, MA).

**Synthetic peptides used for in vitro phosphorylation**

The peptides VRRRQSVELH and VRRRQSVALH have been synthesized using a peptide synthesizer (Model 431-A; Applied Biosystems, Foster City, CA) by Fmoc/tBu chemistry (42).

The purity of the isolated peptide was 95% or more on the basis of peak areas as determined by analytical HPLC. The molecular weights checked with KRATOS MALDI-TOF MS (Shimadzu, Duisburg, Germany) agreed well with the theoretical values within experimental error.

## RESULTS

### Phosphorylation dynamics of AQP2 during maturation from the ER to the vesicular compartment: effect of BFA

Localization and phosphorylation dynamics of AQP2 during maturation from the ER to the vesicular compartment were studied in BFA-treated AQP2-transfected renal CD8 cells (13). BFA is a fungal metabolite that inhibits the secretory pathway by blocking anterograde vesicular transport from the ER and causes redistribution of the cisternae of the Golgi complex into the ER (14–16).

BFA treatment of CD8 cells followed by BFA washout at the indicated times allowed us to follow in parallel AQP2 trafficking and phosphorylation dynamics of newly synthesized AQP2 from the ER to the vesicular compartment. BFA treatment was performed for 16 h, after which time most of the existing AQP2 was expected to be degraded, whereas newly synthesized AQP2 was accumulated in the ER. Figure 1*A* shows the effect induced by BFA incubation (1 μg/ml, 16 h) on AQP2 localization in CD8 cells. For each experimental condition, in the upper part of the panel, a large field of confluent cell is shown and in the bottom part of the panel, a single cell from the field is shown.

In control cells, AQP2 was localized to small intracellular vesicles as described previously (13). Consistent with findings obtained in CHO cells (17), in BFA-treated cells, AQP2 was localized to the ER. In this experimental condition, the lack of staining with the Golgi marker NBD $C_6$-ceramide (NBDC6) confirmed the complete disorganization of the Golgi complex (Fig. 1*A*, inset). After 2 h BFA washout, AQP2 staining was localized in typical large perinuclear structures resembling the reformed Golgi complex. After 4 h BFA washout, the pattern of AQP2 localization was similar to that found in CTR condition, displaying most of the immunoreactivity in small vesicles, distinct from the structures stained by the Golgi marker NBDC6. The fluorescent ceramide analog NBDC6 tends to associate preferentially with the trans-Golgi (18). The lipophilicity of this probe makes it impossible to perform double labeling experiments with AQP2 because the permeabilization steps necessary to introduce anti-AQP2 antibodies extract the lipids.

Studies of the kinetics of AQP2 phosphorylation (Fig. 1*B*) revealed that in control cells both unglycosylated 29 kDa and mature 35-48 kDa glycosylated AQP2 (gly) were phosphorylated. Interestingly, in BFA-treated cells, when almost all AQP2 is localized to the ER, the amount of phosphorylated 29 kDa AQP2 was reduced by nearly 80%. Moreover, in the ER, besides the 29 kDa phosphorylated band, the high mannose (h.m.) 32 kDa form of AQP2 is phosphorylated. After 2 h BFA washout, when newly synthesized AQP2 moves from the ER to the reorganizing Golgi compartment, the amount of phosphorylated 29 kDa AQP2 and of the h.m. glycosylated form of AQP2 increased significantly. This effect was even stronger when the PKA inhibitor H89 was present during BFA washout, a maneuver that should block AQP2 in the Golgi. It is

known, in fact, that H89 impairs budding of vesicles containing newly synthesized proteins from the Golgi (9, 10).

Note that 4 h BFA washout was associated with a significant decrease in the amount of both 29 kDa and 32 kDa phosphorylated AQP2 compared with 2 h BFA washout. This indicates that AQP2 trafficking from Golgi to vesicular storage compartment is associated with a decrease in AQP2 phosphorylation. The means ±SE of the densitometric analysis of the 29 kDa phosphorylated bands normalized for AQP2 abundance assessed by Western blotting in each experiment are reported in Figure 1*B*'.

The h.m. 32 kDa was substituted by the mature 35–48 kDa after a longer BFA washout (8 h). As shown in Figure 1*C*, immunoblotting of AQP2 immunoprecipitated from BFA-treated cells followed by BFA washout (2–8 h) demonstrates that the BFA effect was fully reversible, leading to a 29 kDa and a mature 35–48 kDa glycosylated AQP2. Note that phosphorylation studies cannot be performed at 8 h, because of phosphate degradation.

To verify that the pool of AQP2 studied was entirely newly sinthesized, we carried out pulse-chase experiments. CD8 cells were pulsed with [$^{35}$S] methionine/cysteine for 1 h and chased in the absence (Fig. 2*A*) or in the presence (Fig. 2*B*) of BFA. Quantitation of the radioactivity associated with AQP2 at various times of chase indicated that radioactive AQP2 (both the 29 kDa band and the glycosylated 35–48 kDa band) was maximally detectable at 0 h of chase and gradually degraded at 4, 8, and 16 h of chase, time at which radioactive AQP2 was virtually undetectable (Fig. 2*A*). When BFA was present during the chase time (Fig. 2*B*, +BFA), the time course of radioactive AQP2 degradation in the post-Golgi compartments was similar to that observed in the absence of BFA. As expected, no radioactive AQP2 was immunoprecipitable after BFA washout.

These findings indicate that in CD8 cells, after 16 h of BFA treatment, all the post-Golgi AQP2 is virtually completely degraded and AQP2 present in cells is entirely newly synthesized and accumulated in the ER. Indeed, immunoblotting experiment performed on the same gels exposed for fluorography confirmed that AQP2 immunoprecipitated during BFA treatment was present as 29 kDa band and h.m. 32 kDa band consistent with an accumulation of newly synthetized AQP2 in the ER (data not shown).

We next verified whether AQP2 phosphorylation occurring in the post-ER compartment, probably the Golgi complex, regarded the Ser-256 located in the AQP2 C terminus. To this end, we used an antibody specifically recognizing Ser-256-phosphorylated AQP2 (p-AQP2) (3). Immunolocalization experiments revealed that in control CD8 cells, p-AQP2 was present in intracellular vesicles, displaying a distribution similar to that described by Christensen et al. (4) in renal principal cells (Fig. 3*A*, Ctr). In cells pretreated for 16 h with BFA, a very low staining was visible, indicating that in the ER, AQP2 is weakly phosphorylated at Ser-256 (Fig. 3*A*, BFA). After 2 h of BFA washout, a time at which newly synthesized AQP2 is mainly located in large perinuclear structures likely corresponding to the Golgi complex, the p-AQP2 staining strongly increased, even if the PKA inhibitor H89 was present during the 2 h BFA washout (Fig. 3*A*, 2 h wo and 2 h wo+H89). Prolongation of BFA washout to 4 h resulted in AQP2 transport from the Golgi to the vesicular compartment, with a concomitant decrease in p-AQP2 staining (Fig. 3, 4 h wo).

The phosphorylation dynamics of AQP2 at Ser-256 were semiquantified by Western blotting. Cells were treated under the same experimental conditions described for the immunolocalization experiments reported above, AQP2 was immunoprecipitated, and p-AQP2 at Ser-256 was revealed by immunoblotting.

Results shown in Figure 3*B* showed that AQP2 transition from the ER to the post-ER compartment is associated with a PKA-independent increase in AQP2 phosphorylation at Ser-256 by about twofold. Moreover, the exit of AQP2 from the Golgi compartment was associated with a significant decrease in the amount of both 29 kDa and 32 kDa phosphorylated AQP2.

An alternative strategy was used to accumulate newly sinthesized AQP2 in the Golgi compartment without the use of BFA. It is known that lowering the temperature to 20°C blocks the transport of newly synthesized proteins from the TGN (9). Therefore, AQP2 phosphorylation was analyzed under these experimental conditions. As shown in Figure 3*C*, a significant and reversible increase in AQP2 phosphorylation at Ser-256 during Golgi transition was also obtained in CD8 cells when temperature was lowered to 20°C for 2 h. When cells returned to 37°C for 10 min, the signal for p-AQP2 at Ser-256 was strongly reduced even if compared with control cells. These data are in agreement with those obtained with BFA treatment. Taken together, these data are consistent with the view that a protein kinase able to phosphorylate AQP2 at Ser-256 and located in a post-ER compartment, probably in the Golgi apparatus, is committed to phosphorylate AQP2 at Ser-256.

**AQP2 is a potential substrate for the Golgi casein kinase in vitro**

We therefore searched for the known consensus sequences of protein kinases active on seryl residues (19). The first choice candidate appeared to be the kinase G-CK, which phosphorylates serine and hardly threonine residues (20). A fundamental requirement for this kinase activity is the presence of a glutamyl residue at position +2 with respect to the serine residue (19, 21). Studies by Pinna et al. (22) have indicated the presence of this kinase in a Golgi membrane-enriched fraction purified from lactating mammary gland. G-CK is also expressed in rat liver, spleen, brain, and kidney (22) and belongs to a third class of ubiquitous casein kinases, distinct from CKI and CKII. To investigate whether native AQP2 can be a substrate for G-CK, we first developed synthetic peptides reproducing the AQP2 sequence around Ser-256: VRRRQSVELH, corresponding to the native AQP2 sequence, and VRRRQSVALH, substituted at the crucial +2 position (E to A) and expected not to be phosphorylatable by G-CK. G-CK was purified from rat lactating mammary gland (22) and used to evaluate whether these peptides can be phosphorylated by G-CK. Table 1 shows the kinetic constants for the phosphorylation of the peptides by G-CK and PKA. Whereas the native peptide (VRRRQSVELH) displayed favorable kinetic parameters, the derivative in which the crucial glutamic acid at position +2 was replaced by alanine was almost unaffected by G-CK. In contrast, these two peptides are both excellent substrates for PKA.

**Impaired constitutive phosphorylation of AQP2 in the Golgi might cause AQP2 routing to lysosomes**

A dominant form of nephrogenic diabetes insipidus (NDI), caused by AQP2 mutation E258K and generating a protein that is impaired in its routing to plasma membrane (17, 23, 24), regards

the crucial glutamic acid sitting in the putative G-CK consensus sequence (S-x-E). Therefore, RC.SV3 rabbit cortical collecting duct cells (wild-type CD8 cells) (25) were stably transfected with the cDNA encoding for E258K-AQP2 and S256A-AQP2. Both mutations—the former affecting the hallmark residue for G-CK activity, and the latter implying the target aminoacid for both G-CK and PKA activity—are predicted to impair AQP2 phosphorylation by G-CK.

3-D analysis of cells stained with the anti-AQP2 antibody, obtained by laser scanning confocal microscopy (LSCM), showed that both E258K-AQP2 and S256A-AQP2 did not redistribute upon forskolin stimulation, whereas a clear accumulation of AQP2 on the apical pole was observed in cells expressing wild-type AQP2 (Fig. 4*A*, wt, EK, SA). Western blotting analysis, using AQP2 antibodies, showed that both E258K-AQP2 and S256A-AQP2 were expressed with an efficiency comparable to wild-type AQP2 in CD8 cells, and no apparent difference in the glycosylation pattern was observed for either of the AQP2 mutants (Fig. 4*B*). Staining with the tight junction marker ZO-1 confirmed that both clonal cells are polarized (data not shown) as the wild-type AQP2-transfected CD8 cells (13).

Next, the phosphorylation state of AQP2 in all clonal cell lines was examined. Intact wild-type AQP2-, E258K-AQP2-, and S256A-AQP2-expressing cells were radiolabeled with [$^{32}$P] orthophosphate and left under basal conditions (Fig. 4*C*, CTR) or stimulated with forskolin. Cells were lysed, AQP2 was immunoprecipitated with the specific antibody, and the immunocomplexes were separated by SDS-PAGE. Gels were stained, dried, and exposed for autoradiography (Fig. 4*C*). Under control conditions, the phosphorylation level of AQP2 immunoprecipitated from E258K-AQP2 and S256A-AQP2 was dramatically reduced compared with wild-type AQP2 immunoprecipitated from CD8 cells. Immunoblotting experiments confirmed that equal amounts of AQP2 were immunoprecipitated in all experimental conditions for all cell lines (Fig. 4*C*, W.B.). Moreover, forskolin treatment did not promote any significant increase in AQP2 phosphorylation in intact E258K-AQP2 or in S256A-AQP2-expressing cells (Fig. 4*A* and densitometry in Fig. 4*C*'), whereas a nearly twofold increase in AQP2 phosphorylation was observed in wild-type cells. Note that the E258K-AQP2 mutation does not affect the PKA consensus sequence. The means ±SE of the densitometric analysis of the 29 kDa phosphorylated bands normalized for AQP2 abundance assessed by Western blotting in each experiment are reported in Fig. 4*C*'.

To define the intracellular localization of E258K-AQP2 or S256A-AQP2, we performed double labeling experiments, using different organelle markers. Coimmunolocalization studies using AQP2 antibodies and different markers for Golgi cisternae did not reveal a substantial colocalization (data not shown). In contrast, LSCM of cells double labeled with anti-AQP2 antibody and a monoclonal antibody specific for AC17, a lysosomal resident protein (26), demonstrated that both mutated forms of AQP2 were mainly expressed in lysosomes (Fig. 5*A*). As shown, in wild-type AQP2-expressing cells, AQP2 is localized in discrete vesicles scattered in the cytoplasm, with no significant colocalization with lysosomes. In contrast, both E258K-AQP2 and S256A-AQP2 resulted predominantly expressed in larger structures positive for the lysosome marker (Fig. 5*A*, merge). A more precise analysis of colocalization sites was obtained with Imaris software (see Materials and Methods for details), allowing the visualization of colocalization sites as white spots shown in the right-hand column (Fig. 5*A*', colocalization).

**Phosphorylation dynamics of E258K-AQP2 and S256A-AQP2 during maturation from the ER to the vesicular compartment: effect of BFA**

The detection of low phosphorylation levels of E258K-AQP2 found in basal condition does not exclude that, similar to wt AQP2, this mutant undergoes an increase in phosphorylation during transition from the ER to the Golgi. We therefore analyzed the phosphorylation dynamics of E258K-AQP2 and S256A-AQP2 before reaching the lysosomal compartment in cells pretreated with BFA (Fig. 6*A*, 6*B*). In BFA-treated cells, both E258K-AQP2 and S256A-AQP2 were localized to the ER as for wild-type AQP2, and the lack of staining with NBDC6 confirmed the complete disorganization of the Golgi complex (Fig. 6*A*, 6*B*, insets). After 2 h BFA washout, the Golgi complex was reorganized and both E258K-AQP2 and S256A-AQP2 staining appeared localized in this compartment, consisting of typical large structures, as also observed for wild-type AQP2 (see Fig. 1*A*). After 4 h BFA washout, the pattern of both E258K-AQP2 and S256A-AQP2 localization was indistinguishable from the CTR condition, displaying most of the immunoreactivity in intracellular large vesicles previously identified as lysosomes, distinct from NBDC6-positive structures.

In parallel, studies of the kinetics of E258K-AQP2 and S256A-AQP2 phosphorylation under the same experimental conditions described above revealed no increase in phosphorylation for any mutants after the release from the ER following BFA washout (Fig. 6*C* and densitometry in 6*C'*). Moreover, in contrast with what we observed for wild-type AQP2, no significant increase in either form of mutated AQP2 was detectable when anterograde transport from the ER was carried out in the presence of H89 or when BFA washout was extended to 4 h. Immunoblotting confirmed that equal amounts of AQP2 were loaded for clonal cell line in each condition (Fig. 6C, W.B.). Note that no relative increase in phosphorylation levels was detectable even if autoradiographies were overexposed (data not shown). The means ±SE of the densitometric analysis of the 29 kDa phosphorylated bands normalized for AQP2 abundance assessed by Western blotting in each experiment are reported in Figure 6C'.

Immunoblotting of E258K-AQP2 and S256A-AQP2 immunoprecipitated from BFA-treated cells followed by BFA washout (2–8 h) demonstrated that the modifications in the glycosylation pattern for both mutants were comparable to that observed in wild-type AQP2 (Fig. 6D, 6E). Even for these mutants, the BFA effect was fully reversible and the h.m. 32 kDa was replaced by the mature 35–48 kDa glycosylated form in both cases.

## DISCUSSION

Many secreted proteins become constitutively phosphorylated during their maturation through the secretory pathway, and it is known that phosphorylation events might be key signals involved in the polarized trafficking of proteins. According to this, mutations affecting the kinase's consensus sequence in target proteins might impair protein maturation and functionality.

In this study, we analyzed the phosphorylation dynamics of the vasopressin-regulated water channel AQP2 during its maturation from the ER to the vesicular compartment. In addition, we analyzed whether phosphorylation-defective AQP2 is impaired in its routing in renal cells. AQP2 maturation was analyzed in BFA-treated cells. It is known that BFA causes a reversible redistribution of the cisternae of the Golgi complex into the ER. Cells were treated with BFA for

16 h, allowing the degradation of the existing AQP2 and the accumulation of all newly synthesized AQP2 in the ER.

After BFA washout, both AQP2 trafficking as well as its phosphorylation dynamics during anterograde transport from the ER to the vesicular compartment were followed for 8 h. Phosphorylation experiments revealed that in the ER, both the 29 kDa and the h.m. 32 kDa AQP2 were weakly phosphorylated. After 2 h of BFA washout, a time at which newly synthesized AQP2 was mainly located in the Golgi area, the amount of phosphorylated AQP2 at Ser-256 increased significantly, even if the PKA inhibitor H89 was present during this time. Previous studies in CD8 cells have shown the ability of H89 to prevent both a forskolin-induced increase in AQP2 phosphorylation (12) and RhoA phosphorylation (27).

This indicates that AQP2 transition in the Golgi apparatus is associated with a PKA-independent increase in AQP2 phosphorylation. Prolongation of BFA washout to 4 h resulted in AQP2 transport from the Golgi to the vasopressin-regulated vesicular compartment with a concomitant decrease in AQP2 phosphorylation. It has been reported that functional expression of mutated S256D-AQP2 in MDCK cells (28), mimicking the constitutively phosphorylated AQP2, results in a protein that is routed to the plasma membrane, suggesting that AQP2 dephosphorylation should not be responsible per se for AQP2 exit from the Golgi. Dephosphorylation is probably accomplished by phosphatases associated with AQP2-bearing vesicles (11).

Note that this study describes for the first time the modifications in the AQP2 phosphorylation in parallel with alterations in glycosylation pattern during its maturation. This was possible because CD8 cells express both 29 kDa and the mature 35–48 kDa glycosylated forms, as in native principal cells, whereas in other expression systems, as MDCK cells (28) or LLCPK1 cells (1, 2), wild-type AQP2 is mainly expressed as unglycosylated 29 kDa protein.

Interestingly, we observed that both the 32 kDa AQP2 band, corresponding to the h.m. form of AQP2, and the mature 35–48 kDa glycosylated AQP2 were phosphorylated during AQP2 maturation. Note that even after 4 h BFA washout, the h.m. 32 kDa AQP2 form was still immunoprecipitable and the mature 35–48 kDa glycosylated AQP2 was poorly detectable. This may be due to a partial inhibition of some Golgi enzymes induced by BFA as previously reported (29). Alternatively, although after 2 h BFA washout, the Golgi marker NBDC6 reveals that the Golgi structures are reformed, it cannot be excluded that some Golgi resident proteins, including glycosylation enzymes, might still be retarded in the ER/Golgi hybrid compartment. This possibility is supported by the observation that in CD8 cells, after 2 h BFA washout, antibodies against Golgi markers p58K and giantin failed to recognize a Golgi structure (data not shown), although the Golgi lipid marker stained a well-organized Golgi structure. Immunoprecipitation experiments, however, demonstrated that the mature glycosylated 35–48 kDa AQP2 is expressed after 8 h BFA washout, confirming that the BFA effect is fully reversible. As the last station of the Golgi complex, the TGN plays a pivotal role in sorting proteins to the appropriate membrane destination (see ref 30 for review). Export from the TGN is subjected to control by several kinases (9, 10).

Here, we provide evidence that the vasopressin-sensitive water channel AQP2 is constitutively phosphorylated at Ser-256 during its transition through the Golgi complex by a kinase distinct from PKA that we have tentatively identified as G-CK. In fact, the AQP2 aminoacidic sequence

around Ser-256 also fulfils the consensus sequence of another class of protein kinases, G-CK, found by Lasa et al. (22) in several mammalian tissues. G-CK activity has been described in rat kidney (22) and in rat kidney cell lines (31). G-CK phosphorylates seryl residues specified by an acidic amino acid at position +2. This consensus sequence occurs around AQP2 (RRQSVEL), making it a potential substrate for G-CK, and the same sequence is also a good target for PKA by virtue of the two arginyl residues at positions –2 and –3 (32).

Synthetic peptide reproducing the Ser-256 AQP2 phosphorylation sequence (VRRRQSVELH) was readily phosphorylated in vitro by both PKA and G-CK. A derivative in which the glutamyl residue at position +2 relative to serine was replaced by alanine failed to be phosphorylated by G-CK, whereas it still acted as a PKA substrate. This finding supports the possibility that G-CK is a candidate responsible for the AQP2 phosphorylation that occurs in the Golgi complex.

To investigate whether AQP2 phosphorylation in the Golgi is a physiologically relevant phenomenon, the routing and the phosphorylation of intact wild-type AQP2, E258K-AQP2, responsible for a dominant form of NDI, and S256A-AQP2 were compared in renal cells. These studies led to two key results: First, when compared with wild-type AQP2, transit of mutated E258K-AQP2 and S256A-AQP2 through the Golgi was not associated with an increase in phosphorylation. Second, double labeling experiments revealed that most of the E258K-AQP2 and S256A-AQP2 labeling colocalized with the lysosomal protein AC17.

A possible explanation for the first effect is that in E258K-AQP2 phosphorylation is impaired by the lack of Glu-258, the hallmark residue for G-CK activity, and in S256A-AQP2 because of the absence of the Ser-256 itself. The second observation might be a physiological consequence of the first: AQP2 phosphorylation in the Golgi may be required for subsequent AQP2 sorting to the intracellular vesicles, and, consequently, phosphorylation-defective AQP2 is routed to lysosomes. It has to be recognized however that although a consistent colocalization with lysosomes was observed, we cannot exclude the possiblity that mutated AQP2 also partially accumulates in the TGN, which we cannot detect in CD8 cells because of the lack of antibodies cross-reacting with the TGN on our cells. Indeed, Hirano et al. (33) recently reported that in rat hepatocytes stably transfected with E258K-AQP2, this protein is retained in a Golgi apparatus/lysosome compartment.

Our results on the lysosomal localization of S256A-AQP2 in CD8 cells are not in agreement with previous observations showing that in MDCK cells (28) and in LLCPK1 cells (1) the AQP2-S256A appeared predominantly expressed in a vesicular compartment, which however has not been precisely identified by double labeling experiments. This possible discrepancy might be due to the different renal cell lines used, probably sharing a different pattern of regulatory proteins.

On the other hand, analysis of the phosphorylation dynamics and the localization of E258K-AQP2 and S256A-AQP2 during maturation from the ER to the vesicular compartment in BFA-treated cells confirmed that E258K-AQP2 and S256A-AQP2 transited through the Golgi complex before sorting to lysosomes. This strongly supports the view that the inability to phosphorylate AQP2 at Ser-256 in the Golgi limits the sorting to the regulatory vesicular compartment, thus resulting in routing to lysosomes. Conversely, phosphorylation at Ser-256 directs AQP2 to the correct vesicular compartment (see proposed model in Fig. 7)

Consistent with this hypothesis, we observed that activation of PKA in intact E258K-AQP2 and S256A-AQP2 cells promoted neither relocation of mutated AQP2 nor a significant increase in phosphorylation. This result is expected for the S256A-AQP2 mutant, as Ser-256 is the target for PKA. In contrast, in E258K-AQP2 mutant, the absence of Glu-258 does not affect the PKA consensus sequence. The implication of this observation is that PKA activity is required downstream from G-CK-dependent AQP2 phosphorylation to allow the apical insertion of the water channel. This also implies that activated PKA cannot reverse the lack of activity of G-CK during transition through the Golgi of the E258K-AQP2.

Together, these results strongly support the concept that a compartmentalization of kinases involved in regulating AQP2 trafficking should exist in renal cells. Indeed, findings by Klussmann et al. (34) confirmed that PKA tethering to subcellular compartments is necessary for cAMP-dependent AQP2 translocation. PKA-dependent AQP2 phosphorylation at Ser-256 would be restricted to the vesicular compartments for short-term regulation of AQP2 insertion. Conversely, PKA-independent AQP2 phosphorylation at Ser-256 occurs in the Golgi network, probably required for the exit of AQP2 from this organelle.

The role of phosphorylation as a routing determinant for membrane proteins has been well established (35). Many secretory proteins become phosphorylated during their movement through the secretory pathway. In MDCK cells, the polymeric immunoglobulin receptor is targeted from the TGN to apical and basolateral endosomes, and phosphorylation of a serine residue in the cytoplasmic tail of the receptor is implicated in this process (36). Phosphorylation of target proteins at a single serine residue may trigger the binding of adaptor proteins involved in vesicular transport. Among these proteins, the 14-3-3 family has been suggested to function as adaptor proteins that can stabilize protein-protein interactions. 14-3-3 specifically binds phosphoserines in the sequence context R(S)X1,2SpX(P) (where X represents any amino acid, Sp represents phosphoserine, and parentheses represent common but not mandatory amino acid residues). The cytoplasmic tail sequence of AQP2 fits well with this motif.

These proteins were found associated with the Golgi complex in mammalian cells (37) and in MDCK cells (38). Analysis of functional expression of mutated AQP2 causing NDI, a disease in which the kidney does not respond to AVP, gives strong support to our hypothesis. First, the disease model of dominant NDI caused by AQP2 mutation E258K (23) affects the crucial glutamic acid of the G-CK consensus sequence (S-x-E). The findings presented here provide some clues to understanding the molecular basis of this particular form of NDI, in which the phenotype is caused by an impaired routing of AQP2. The prediction is that the lack of Glu-258 will prevent phosphorylation of AQP2 by G-CK, a signal that might play an essential role in sorting AQP2 to the regulated vesicular compartment.

Conversely, one would expect that mutation in the PKA consensus sequence not affecting the G-CK consensus sequence would generate a protein that is constitutively phosphorylated by G-CK but not able to translocate in response to elevation of intracellular cAMP, leading to an NDI phenotype. Indeed, a family with dominant NDI was recently identified in which an AQP2 gene mutation was found encoding R254L-AQP2, a mutation that destroys the PKA consensus sequence but not the putative G-CK consensus sequence. Note that when expressed in MDCK cells, R254L-AQP2 was retained within the cell and was phosphorylated at Ser-256, supporting the hypothesis that Ser-256 in AQP2 is phosphorylated by kinases other than PKA (39).

In conclusion, the present work demonstrates for the first time that intracellular trafficking of AQP2 from the ER to the regulated vesicular compartment is parallel to multistep phosphorylation dynamics. The detailed analysis of AQP2 phosphorylation during its maturation provides insight in understanding the molecular basis of some forms of NDI caused by naturally occurring mutations in the AQP2 water channel gene .

## ACKNOWLEDGMENTS

We thank E. J. Kamsteeg, P. Savelkoul, and P. M. Deen (University of Nijmegen, The Netherlands) for kindly providing the constructs pCDNA3-AQP2-E258 and pCB6-S256A-AQP2. We also thank Dr. E. Rodriguez-Boulan (Cornell University, Cornell, NY) for kindly providing antibodies against AC17, Dr. Mario Ventura for experimental assistance, and our colleague Anthony Green for proofreading and providing linguistic advice. This work was supported by a grant from the L.A.G. (Laboratorio Analisi del Gene, cluster C03), from the Italian Ministero della Ricerca Scientifica e Tecnologica (MURST, PRIN project), from the Karen Elise Jensen Foundation, from the Commission of the European Union (EU-Biotech), and from the Danish Medical Research Council.

## REFERENCES

1. Katsura, T., Gustafson, C. E., Ausiello, D. A., and Brown, D. (1997) Protein kinase A phosphorylation is involved in regulated exocytosis of aquaporin-2 in transfected LLC-PK1 cells. *Am. J. Physiol.* **272,** F817–F822

2. Fushimi, K., Sasaki, S., and Marumo, F. (1997) Phosphorylation of serine 256 is required for cAMP-dependent regulatory exocytosis of the aquaporin-2 water channel. *J. Biol. Chem.* **272,** 14800–14804

3. Nishimoto, G., Zelenina, M., Li, D., Yasui, M., Aperia, A., Nielsen, S., and Nairn, A. C. (1999) Arginine vasopressin stimulates phosphorylation of aquaporin-2 in rat renal tissue. *Am. J. Physiol.* **276,** F254–F259

4. Christensen, B. M., Zelenina, M., Aperia, A., and Nielsen, S. (2000) Localization and regulation of PKA-phosphorylated AQP2 in response to V2-receptor agonist/antagonist treatment. *Am. J. Physiol.* **278,** F29–F42

5. Kamsteeg, E. J., Heijnen, I., van Os, C. H., and Deen, P. M. (2000) The Subcellular Localization of an Aquaporin-2 Tetramer Depends on the Stoichiometry of Phosphorylated and Nonphosphorylated Monomers. *J. Cell Biol.* **151,** 919–930

6. Simon, J. P., Ivanov, I. E., Shopsin, B., Hersh, D., Adesnik, M., and Sabatini, D. D. (1996) The in vitro generation of post-Golgi vesicles carrying viral envelope glycoproteins requires an ARF-like GTP-binding protein and a protein kinase C associated with the Golgi apparatus. *J. Biol. Chem.* **271,** 16952–16961

7. Jones, S. M., Alb, J. G., Jr., Phillips, S. E., Bankaitis, V. A., and Howell, K. E. (1998) A phosphatidylinositol 3-kinase and phosphatidylinositol transfer protein act synergistically in

formation of constitutive transport vesicles from the trans-Golgi network. *J. Biol. Chem.* **273,** 10349–10354

8. Molloy, S. S., Thomas, L., Kamibayashi, C., Mumby, M. C., and Thomas, G. (1998) Regulation of endosome sorting by a specific PP2A isoform. *J. Cell Biol.* **142,** 1399–1411

9. Muniz, M., Martin, M. E., Hidalgo, J., and Velasco, A. (1997) Protein kinase A activity is required for the budding of constitutive transport vesicles from the trans-Golgi network. *Proc. Natl. Acad. Sci. USA* **94,** 14461–14466

10. Martin, M. E., Hidalgo, J., Rosa, J. L., Crottet, P., and Velasco, A. (2000) Effect of protein kinase A activity on the association of ADP-ribosylation factor 1 to golgi membranes. *J. Biol. Chem.* **275,** 19050–19059

11. Lande, M. B., Jo, I., Zeidel, M. L., Somers, M., and Harris, H. W., Jr. (1996) Phosphorylation of aquaporin-2 does not alter the membrane water permeability of rat papillary water channel-containing vesicles. *J. Biol. Chem.* **271,** 5552–5557

12. Valenti, G., Procino, G., Carmosino, M., Frigeri, A., Mannucci, R., Nicoletti, I., and Svelto, M. (2000) The phosphatase inhibitor okadaic acid induces AQP2 translocation independently from AQP2 phosphorylation in renal collecting duct cells. *J. Cell Sci.* **113,** 1985–1992

13. Valenti, G., Frigeri, A., Ronco, P. M., D'Ettorre, C., and Svelto, M. (1996) Expression and functional analysis of water channels in a stably AQP2- transfected human collecting duct cell line. *J. Biol. Chem.* **271,** 24365–24370

14. Pelham, H. R. (1991) Multiple targets for brefeldin A. *Cell* **67,** 449–451

15. Sciaky, N., Presley, J., Smith, C., Zaal, K. J., Cole, N., Moreira, J. E., Terasaki, M., Siggia, E., and Lippincott-Schwartz, J. (1997) Golgi tubule traffic and the effects of brefeldin A visualized in living cells. *J. Cell Biol.* **139,** 1137–1155

16. Chardin, P., and McCormick, F. (1999) Brefeldin A: the advantage of being uncompetitive. *Cell* **97,** 153–155

17. Tamarappoo, B. K., Yang, B., and Verkman, A. S. (1999) Misfolding of mutant aquaporin-2 water channels in nephrogenic diabetes insipidus. *J. Biol. Chem.* **274,** 34825–34831

18. Pagano, R. E., Sepanski, M. A., and Martin, O. C. (1989) Molecular trapping of a fluorescent ceramide analogue at the Golgi apparatus of fixed cells: interaction with endogenous lipids provides a trans-Golgi marker for both light and electron microscopy. *J. Cell Biol.* **109,** 2067–2079

19. Pinna, L. A., and Ruzzene, M. (1996) How do protein kinases recognize their substrates? *Biochim. Biophys. Acta* **1314,** 191–225

20. Meggio, F., Boulton, A. P., Marchiori, F., Borin, G., Lennon, D. P., Calderan, A., and Pinna, L. A. (1988) Substrate-specificity determinants for a membrane-bound casein kinase of lactating mammary gland. A study with synthetic peptides. *Eur. J. Biochem.* **177,** 281–284

21. Lasa-Benito, M., Marin, O., Meggio, F., and Pinna, L. A. (1996) Golgi apparatus mammary gland casein kinase: monitoring by a specific peptide substrate and definition of specificity determinants. *FEBS Lett.* **382,** 149–152

22. Lasa, M., Marin, O., and Pinna, L. A. (1997) Rat liver Golgi apparatus contains a protein kinase similar to the casein kinase of lactating mammary gland. *Eur. J. Biochem.* **243,** 719–725

23. Mulders, S. M., Bichet, D. G., Rijss, J. P., Kamsteeg, E. J., Arthus, M. F., Lonergan, M., Fujiwara, M., Morgan, K., Leijendekker, R., van der Sluijs, P., et al. (1998) An aquaporin-2 water channel mutant which causes autosomal dominant nephrogenic diabetes insipidus is retained in the Golgi complex. *J. Clin. Invest.* **102,** 57–66

24. Kamsteeg, E. J., Wormhoudt, T. A., Rijss, J. P., van Os, C. H., and Deen, P. M. (1999) An impaired routing of wild-type aquaporin-2 after tetramerization with an aquaporin-2 mutant explains dominant nephrogenic diabetes insipidus. *EMBO J.* **18,** 2394–2400

25. Vandewalle, A., Lelongt, B., Geniteau-Legendre, M., Baudouin, B., Antoine, M., Estrade, S., Chatelet, F., Verroust, P., Cassingena, R., and Ronco, P. (1989) Maintenance of proximal and distal cell functions in SV40-transformed tubular cell lines derived from rabbit kidney cortex. *J. Cell. Physiol.* **141,** 203–221

26. Nabi, I. R., Le Bivic, A., Fambrough, D., and Rodriguez-Boulan, E. (1991) An endogenous MDCK lysosomal membrane glycoprotein is targeted basolaterally before delivery to lysosomes. *J. Cell Biol.* **115,** 1573–1584

27. Tamma, G., Klussmann, E., Procino, G., Svelto, M., Rosenthal, W., and Valenti, G. (2003) cAMP induced AQP2 translocation is associated with RhoA inhibition through RhoA phosphorylation and interaction with RhoGDI. *J. Cell Sci.* **116,** 1519–1525.

28. Van Balkom, B. W., Savelkoul, P. J., Markovich, D., Hofman, E., Nielsen, S., Van Der Sluijs, P., and Deen, P. M. (2002) The role of putative phosphorylation sites in the targeting and shuttling of the Aquaporin-2 water channel. *J. Biol. Chem.* **277,** 41473–41479.

29. Perkel, V. S., Miura, Y., and Magner, J. A. (1989) Brefeldin A inhibits oligosaccharide processing of glycoproteins in mouse hypothyroid pituitary tissue at several subcellular sites. *Proc. Soc. Exp. Biol. Med.* **190,** 286–293

30. Donaldson, J. G., and Lippincott-Schwartz, J. (2000) Sorting and signaling at the Golgi complex. *Cell* **101,** 693–696

31. Price, P. A., Rice, J. S., and Williamson, M. K. (1994) Conserved phosphorylation of serines in the Ser-X-Glu/Ser(P) sequences of the vitamin K-dependent matrix Gla protein from shark, lamb, rat, cow, and human. *Protein Sci.* **3,** 822–830

32. Kennelly, P. J., and Krebs, E. G. (1991) Consensus sequences as substrate specificity determinants for protein kinases and protein phosphatases. *J. Biol. Chem.* **266,** 15555–15558

33. Hirano, K., Roth, J., Zuber, C., and Ziak, M. (2002) Expression of a mutant ER-retained polytope membrane protein in cultured rat hepatocytes results in Mallory body formation. *Histochem. Cell Biol.* **117,** 41–53

34. Klussmann, E., Maric, K., Wiesner, B., Beyermann, M., and Rosenthal, W. (1999) Protein kinase A anchoring proteins are required for vasopressin- mediated translocation of aquaporin-2 into cell membranes of renal principal cells. *J. Biol. Chem.* **274,** 4934–4938

35. Okamoto, C. T., Song, W., Bomsel, M., and Mostov, K. E. (1994) Rapid internalization of the polymeric immunoglobulin receptor requires phosphorylated serine 726. *J. Biol. Chem.* **269,** 15676–15682

36. Orzech, E., Cohen, S., Weiss, A., and Aroeti, B. (2000) Interactions between the exocytic and endocytic pathways in polarized Madin-Darby canine kidney cells. *J. Biol. Chem.* **275,** 15207–15219

37. Leffers, H., Madsen, P., Rasmussen, H. H., Honore, B., Andersen, A. H., Walbum, E., Vandekerckhove, J., and Celis, J. E. (1993) Molecular cloning and expression of the transformation sensitive epithelial marker stratifin. A member of a protein family that has been involved in the protein kinase C signalling pathway. *J. Mol. Biol.* **231,** 982–998

38. Fiedler, K., Kellner, R., and Simons, K. (1997) Mapping the protein composition of trans-Golgi network (TGN)-derived carrier vesicles from polarized MDCK cells. *Electrophoresis* **18,** 2613–2619

39. de Mattia, F., Savelkoul, P. W. M., Nielsen, S., Oksche, A., and Deen, P. M. T. (2002) An impaired routing of wild-type aquaporin-2/AQP2-R254L complexes explains dominant nephrogenic diabetes insipidus, but is independent from AQP2 phosphorylation. In *ASN 35th Annual Meeting*, Pennsylvania Convention Center, Philadelphia, PA

40. Brunati, A. M., Contri, A., Muenchbach, M., James, P., Marin, O., and Pinna, L. A. (2000) GRP94 (endoplasmin) co-purifies with and is phosphorylated by Golgi apparatus casein kinase. *FEBS Lett.* **471,** 151–155

41. Meggio, F., Donella Deana, A., Ruzzene, M., Brunati, A. M., Cesaro, L., Guerra, B., Meyer, T., Mett, H., Fabbro, D., Furet, P., et al. (1995) Different susceptibility of protein kinases to staurosporine inhibition. Kinetic studies and molecular bases for the resistance of protein kinase CK2. *Eur. J. Biochem.* **234,** 317–322

42. Fields, G. B., and Noble, R. L. (1990) Solid phase peptide synthesis utilizing 9-fluorenylmethoxycarbonyl amino acids. *Int. J. Pept. Protein Res.* **35,** 161–214

*Received October 29, 2003; accepted June 19, 2003.*

## Table 1

### Phosphorylation assay of AQP2 peptides by G-CK and PKA

| | **G-CK** | | **PKA** | |
|---|---|---|---|---|
| AQP2 peptides | Vmax (cpm) | Km (μM) | Vmax (cpm) | Km (μM) |
| VRRRQSVELH (relative) | 6354 | 186 | 345,000 | 0.8 |
| VRRRQSVALH (+2 subst.) | nd | nd | 330,000 | 1 |

The peptides VRRRQSVELH and VRRRQSVALH reproducing the AQP2 C-terminus were in vitro phosphorylated by purified G-CK and PKA catalytic subunit. Kinetic parameters for peptide phosphorylation are reported (Vmax, Km). Whereas the native peptide (VRRRQSVELH) displayed favorable kinetic parameters, the derivative substituted at position +2 was almost unaffected by G-CK (nd, not detectable). Both peptides are excellent substrates for PKA.

**Fig. 1**

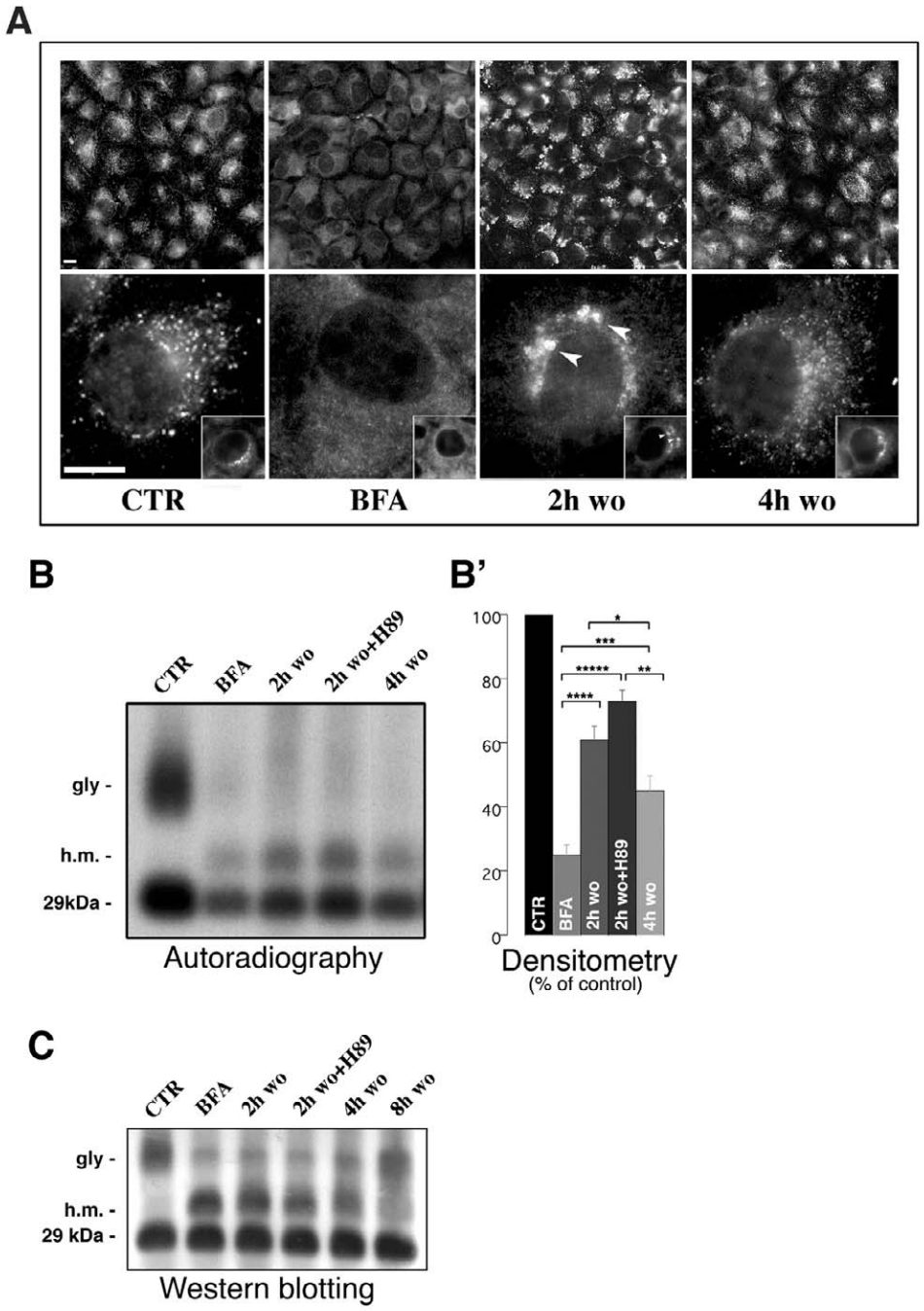


**Figure 1. Immunolocalization and phosphorylation dynamics of newly synthesized AQP2 during maturation from the ER to the vesicular compartment in CD8 cells. *A)*** CD8 cells were left under basal conditions (CTR), treated with BFA (1µg/ml, 16 h) or treated with BFA followed by BFA washoutfor 2 h (2 h wo) or for 4 h (4 h wo). Cells were fixed and stained with AQP2 antibody or with the Golgi marker NBDC6 (inset). At the top of the panel, a large field of confluent cells is shown, and at the bottom, a representative cell is shown. Bars, 10 µm. ***B)*** Cells grown on Petri dishes were treated with BFA as described above. Cells were then labeled with [$^{32}$P] orthophosphate, and BFA was washed out for 2 h in the absence (2 h wo) or in the presence of 30 µM H89 (2 h wo+H89) and for 4 h (4 h wo). Cells were lysed, AQP2 was immunoprecipitated, and an equivalent amount of proteins was separated by SDS-PAGE. Gels were dried and exposed for autoradiography. ***B')*** Mean ±SE of the densitometric analysis performed on the 29 KDa AQP2 band obtained by autoradiography for each experimental condition from three independent experiments. ***C)*** Equal amounts of AQP2 immunoprecipitated from BFA-treated cells followed by BFA washout (2–8 h) were immunoblotted using anti-AQP2 antibodies. *$P$<0.05; **$P$<0.01; ***$P$<0.005; ****$P$<0.001; *****$P$<0.0001 ( Student's $t$ test for paired data).

**Fig. 2**

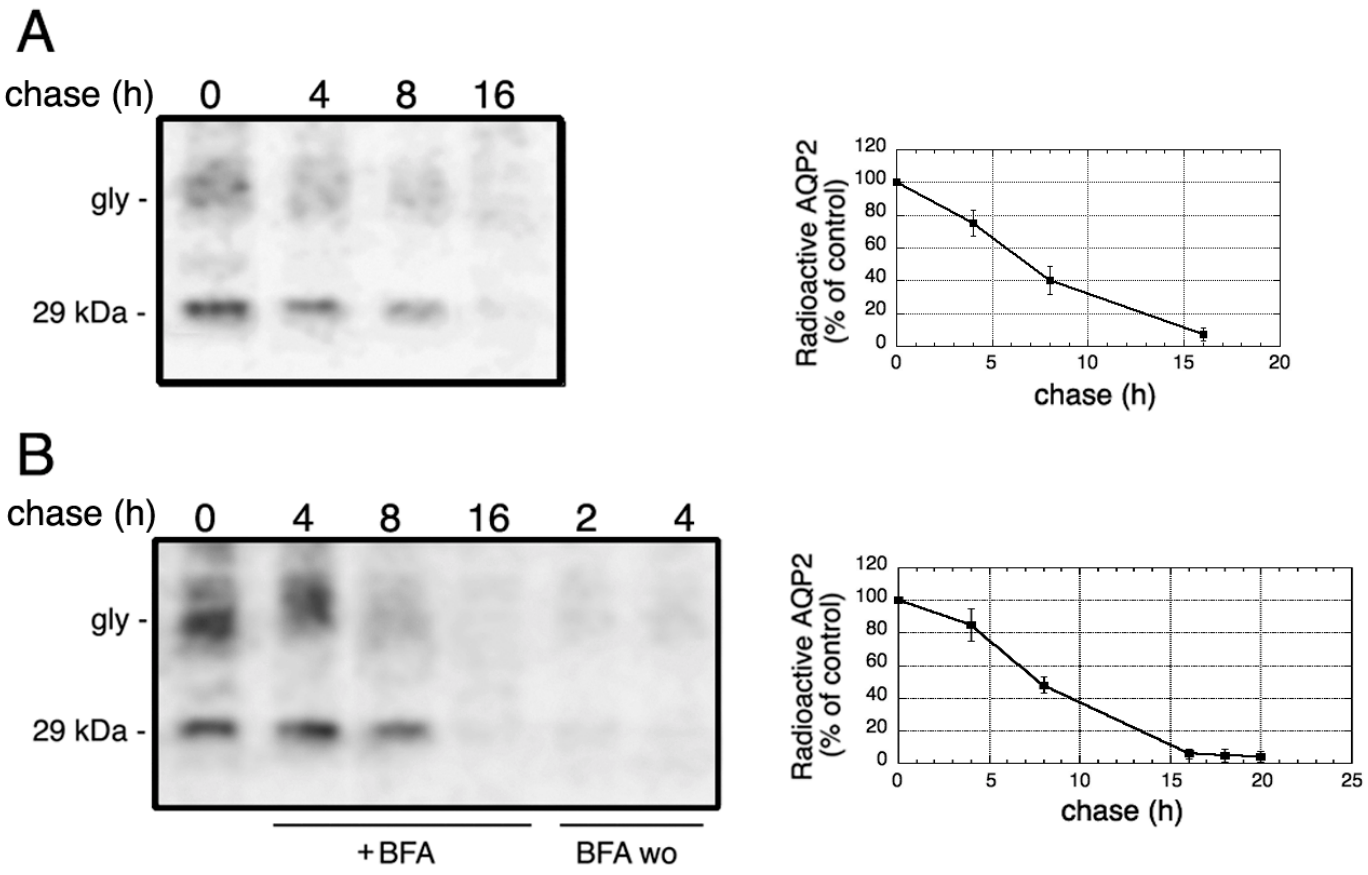


**Figure 2. Pulse chase experiments.** Subconfluent monolayers of CD8 cells were pulse-labeled with 150 μCi/ml of [$^{35}$S] methionine/cysteine for 1 h at 37°C. ***A)*** Cells were then chased in complete medium supplemented with 5 mM of L-methionine and 5 mM of L-cysteine for 0, 4, 8, and 16 h. ***B)*** Where indicated, BFA (1 μg/ml) was added during the chase time. After 16 h of BFA treatment, the drug was washed out for 2–4 h. At the indicated time, cells were lysed and AQP2 was immunoprecipitated and visualized by fluorography. The time course of radioactive AQP2 degradation was not different in BFA- vs. non-BFA-treated cells. Mean ±SE of the densitometric analysis performed on the 29 KDa AQP2 band for each experimental condition from three independent experiments is reported on the right of each panel.

**Fig. 3**

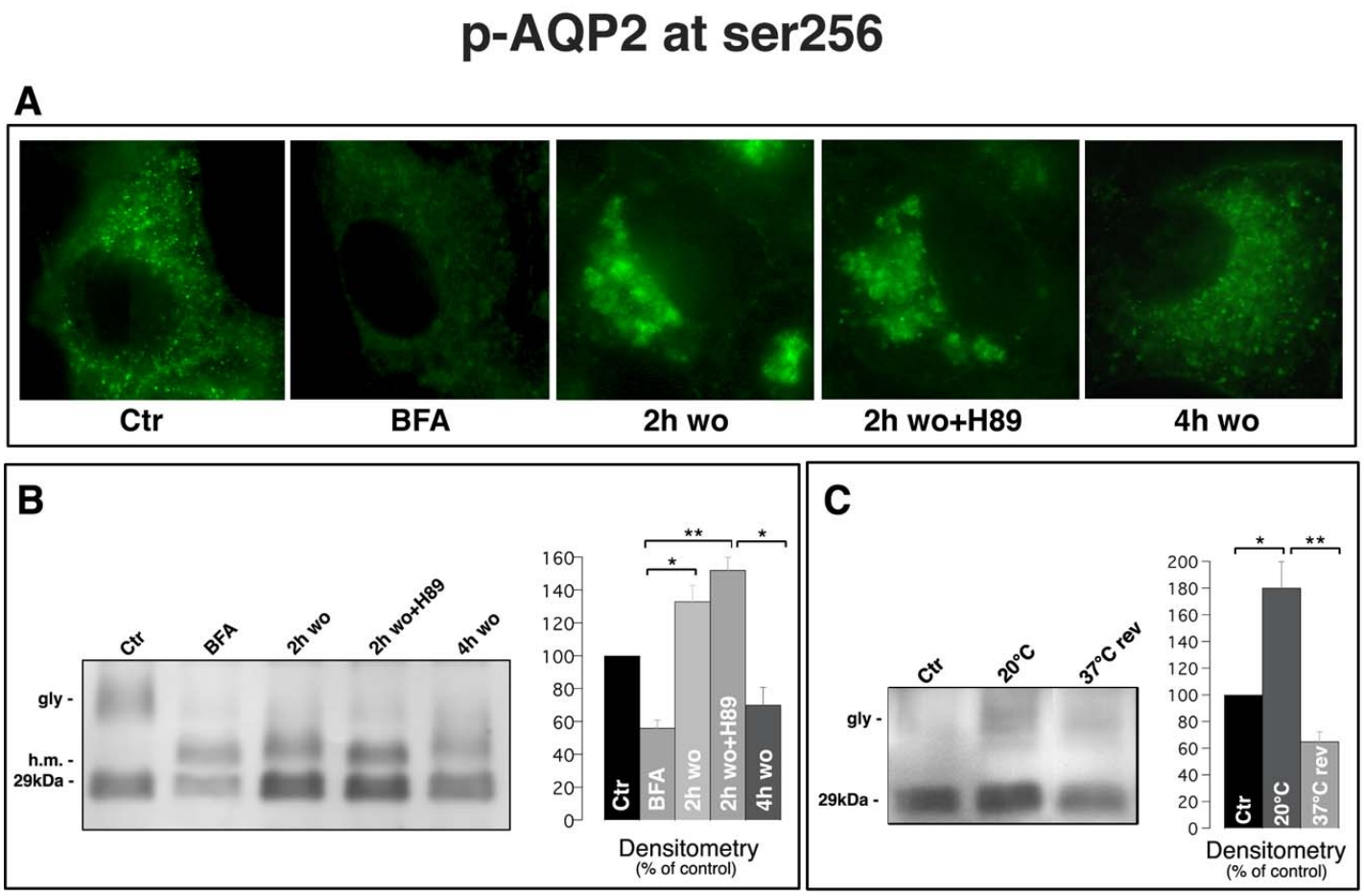


**Figure 3. AQP2 is phosphorylated at Ser-256 during transition in the Golgi complex. *A)*** CD8 cells grown on coverslips were left under basal conditions (CTR), treated with BFA (1 µg/ml, 16 h), treated with BFA followed by BFA washout for 2 h in the absence (2 h wo) or in the presence of H89 (2 h wo+H89) and for 4 h (4 h wo). Cells were fixed and stained with an antibody specifically recognizing p-AQP2 at Ser-256. ***B)*** CD8 were treated as described above and then lysed, and AQP2 was immunoprecipitated and separated by SDS-PAGE. Blots were probed by immunoblotting using antibody anti p-AQP2 at Ser-256. Mean ±SE of the densitometric analysis performed on the 29 KDa AQP2 band for each experimental condition from three independent experiments is reported. **P*<0.001; ***P*<0.0001 (Student's *t* test for paired data). ***C)*** Cells were left untreated (Ctr), kept at 20°C for 2 h (20°C), and returned at 37°C for 10 min (37°C rev.) Immunoprecipitated AQP2 was probed with antibody anti-p-AQP2 at Ser-256. Densitometric analysis is reported on the right. **P*<0.005; ***P*<0.001 (Student's *t* test for paired data).

**Fig. 4**

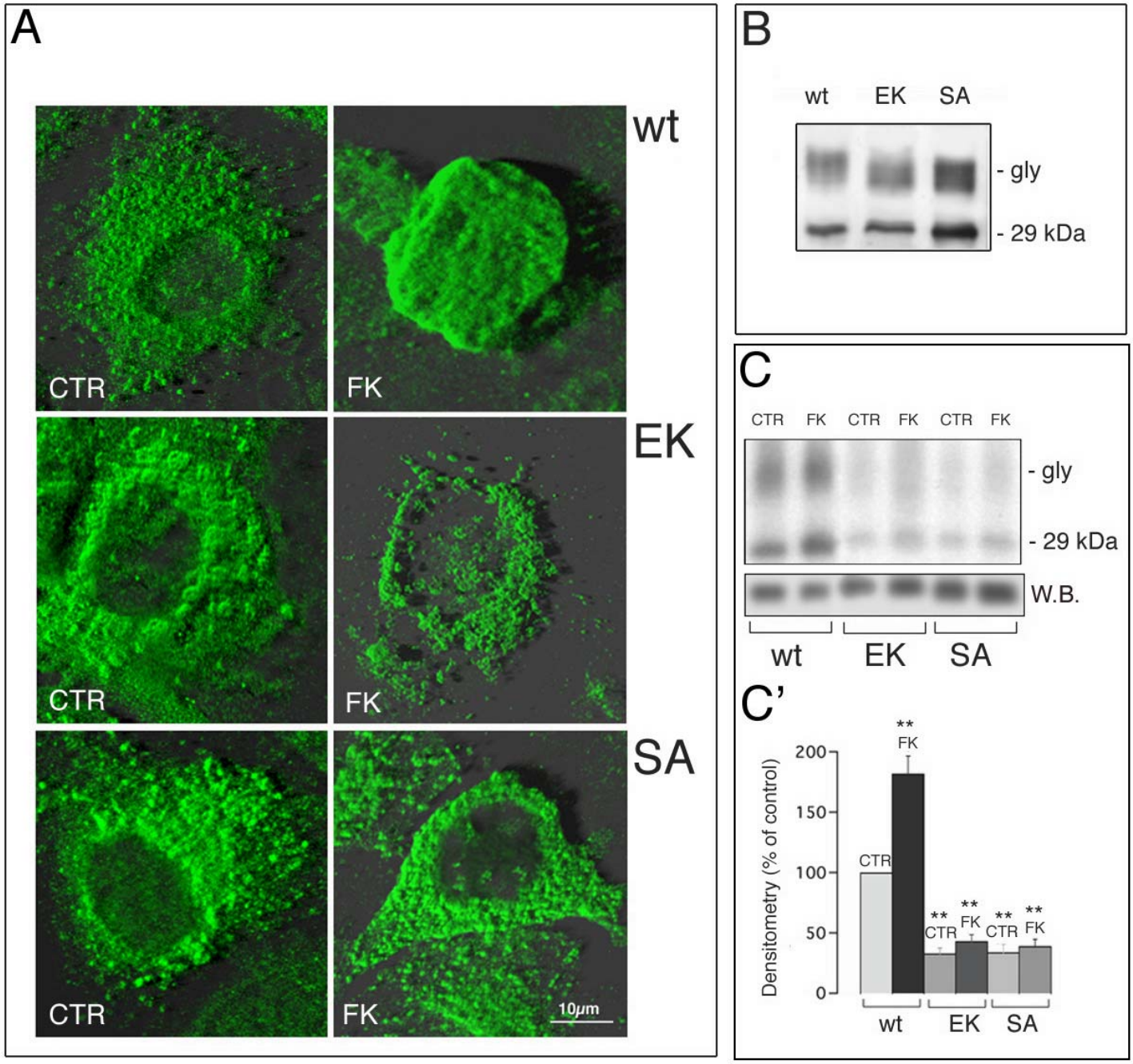


**Figure 4. Immunolocalization and phosphorylation state of wild-type AQP2, E258K-AQP2, and S256A-AQP2.** ***A*)** The 3-D reconstruction of wild-type AQP2 (wt), E258K-AQP2 (EK), and S256A-AQP2 (SA) transfected cells probed with anti-AQP2 affinity purified antibodies. Cells grown on coverslips were left under control conditions (CTR) or stimulated with $10^{-4}$ M forskolin (FK) for 15 min. Fixed cells were probed with AQP2 and stained with anti-rabbit IgG Alexa Fluor 488. ***B)*** Western blotting analysis of wild-type AQP2 (wt), E258K-AQP2 (EK), and S256A-AQP2 (SA) cell lysates probed with AQP2 affinity purified antibodies. ***C)*** Intact cells expressing wild-type AQP2 (wt), E258K-AQP2 (EK), or S256A-AQP2 (SA) were labeled with [$^{32}$P] orthophosphate and left under basal condition (CTR) or stimulated with forskolin (FK). Cells were lysed, AQP2 was immunoprecipitated, and equivalent amount of proteins were separated by SDS-PAGE. Gels were dried and exposed for autoradiography. The amount of immunoprecipitated AQP2 was controlled by Western blotting (W.B.). ***C')*** Means ± SE of the densitometric analysis of the 29 KDa AQP2 phosphorylated bands normalized for AQP2 abundance assessed by Western blotting in each experiment from three independent experiments. ***P*<0.01 ( Student's *t* test for paired data).

**Fig. 5**

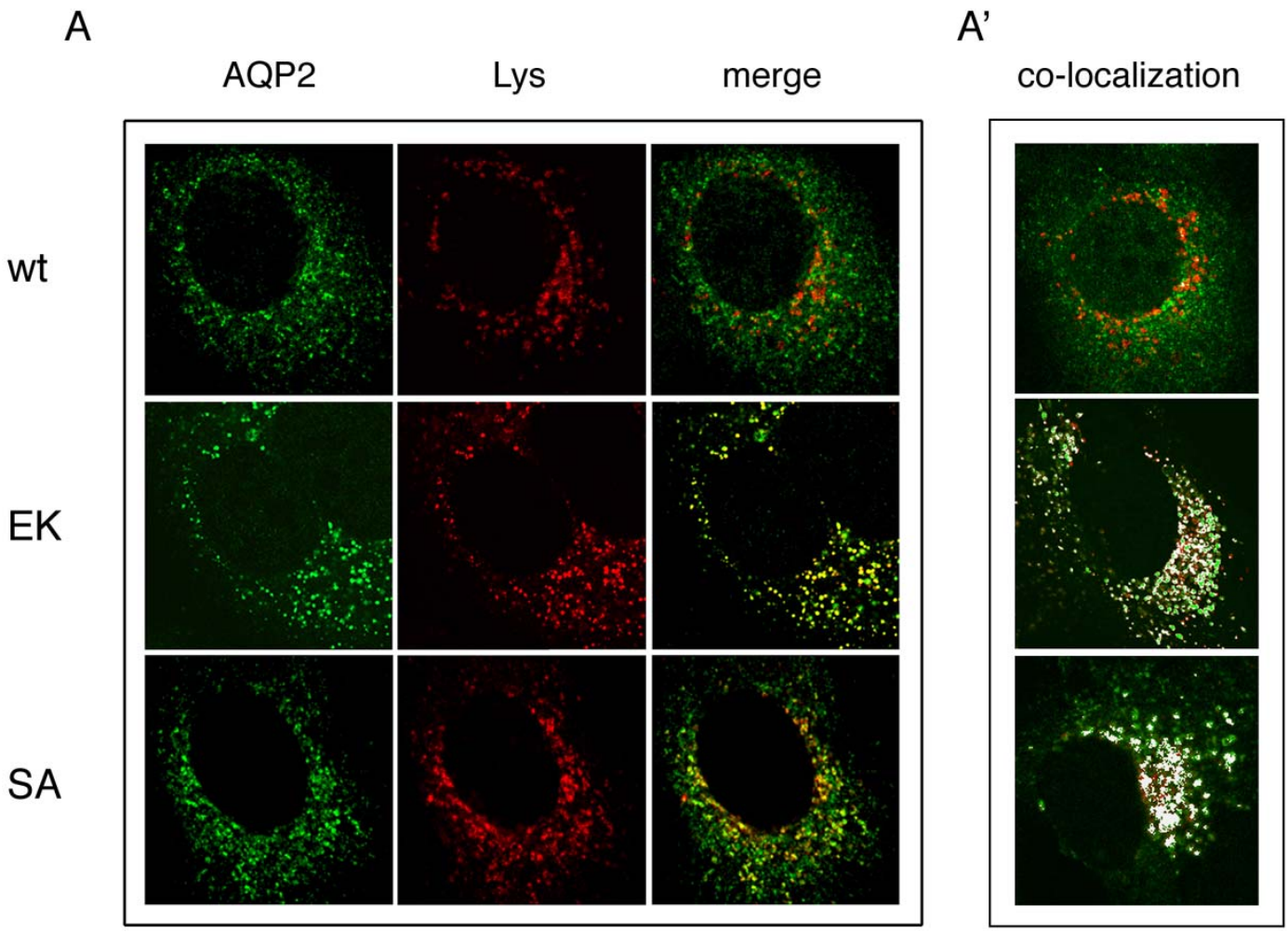


**Figure 5. Co-localization of AQP2, E258K-AQP2 and S256A-AQP2 with the lysosomal marker AC17. *A*)** Confocal analysis of cells expressing wild-type AQP2 (wt), E258K-AQP2 (EK), and S256A-AQP2 (SA) double labeled with AQP2 (green color) and with the lysosomal marker AC17 (red color). ***A'*)** A more precise analysis of co-localization sites was obtained with the Imaris software. White color corresponds to the individual picture localization where the signal of each channel (red and green) falls inside a certain intensity range simultaneously.

**Fig. 6**

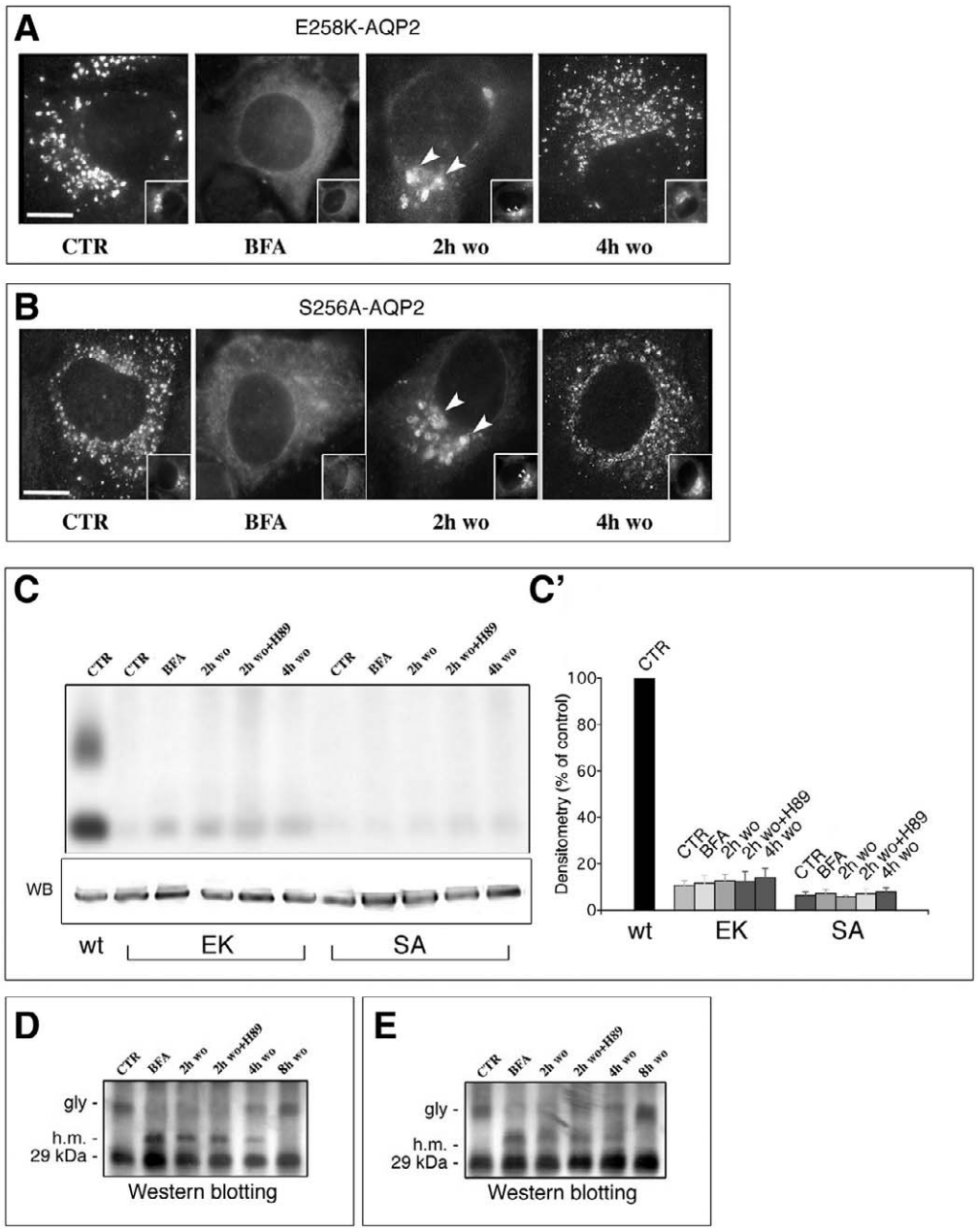


**Figure 6. Maturation and phosphorylation dynamics of newly synthesized E258K-AQP2 and S256A-AQP2.** Cells expressing E258K-AQP2 (***A***) and S256A-AQP2 (***B***) were left under basal condition (CTR), treated with BFA (1µg/ml, 16 h), or treated with BFA followed by BFA washout for 2 h (2 h wo) or for 4 h (4 h wo). Cells were fixed and stained with AQP2 antibody or with the Golgi marker NBDC6 (inset). Bar, 10 µm. ***C)*** Cells expressing AQP2 (wt), E258K-AQP2 (EK), and S256A-AQP2 (SA) were grown on Petri dishes and left under control conditions or pretreated with BFA (1µg/ml, 16 h). Cells were then labeled with [$^{32}$P] orthophosphate, and BFA was washed out for 2 h in the absence (2 h wo) or in the presence of 30 µM H89 (2 h wo+H89) and for 4 h (4 h wo). Cells were lysed, AQP2 was immunoprecipitated, and equivalent amounts of proteins were separated by SDS-PAGE. Gels were dried and exposed for autoradiography. Western blotting analysis of immunoprecipitated proteins (W.B.) confirmed that equal amount of AQP2 proteins were immunoprecipitated in each experimental condition and revealed by autoradiography. ***C')*** Means ±SE of the densitometric analysis of the 29 KDa AQP2 phosphorylated bands normalized for AQP2 abundance assessed by Western blotting in each experiment from three independent experiments. Western blotting of E258K-AQP2 (***D***) and S256A-AQP2 (***E***) immunoprecipitated from control or BFA-treated cells followed by BFA washout (2–8 h) and probed with anti-AQP2 antibodies.

**Fig. 7**

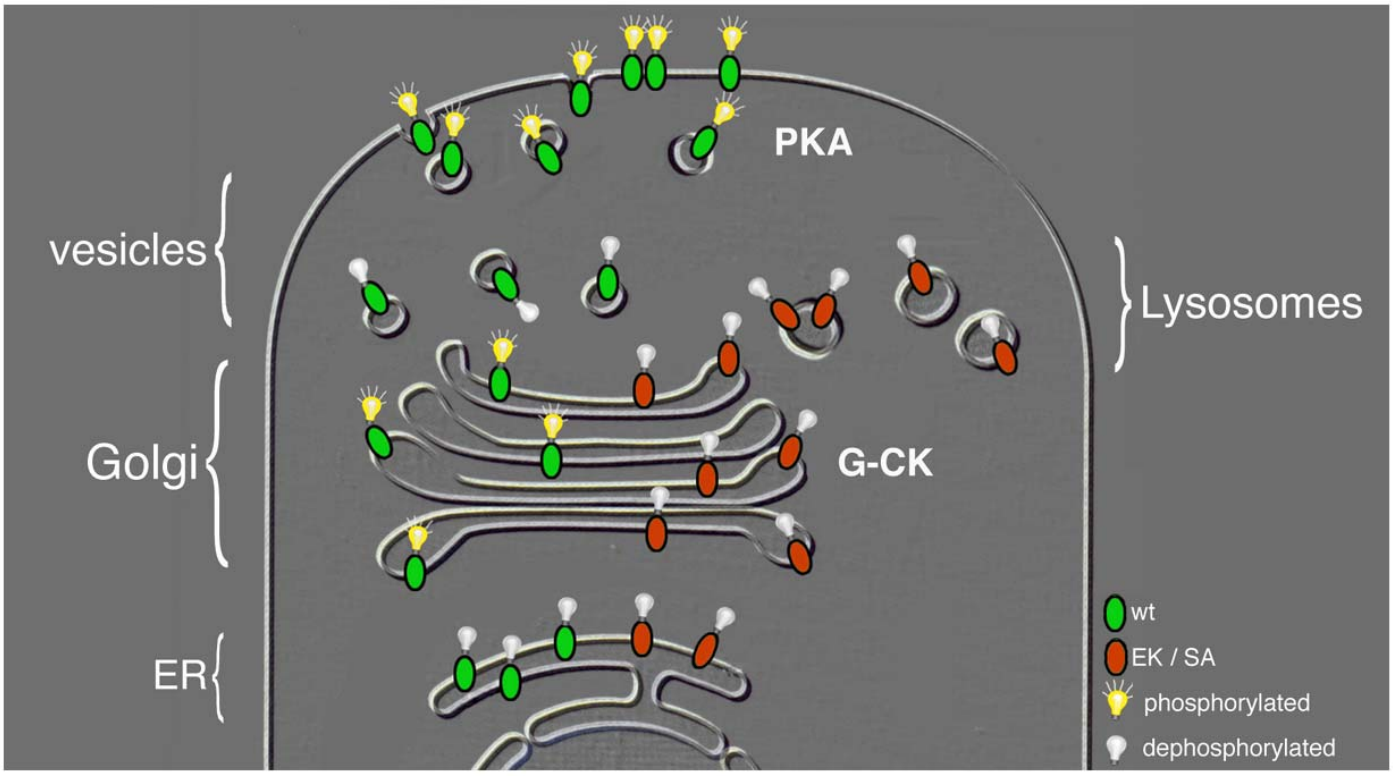


**Figure 7. Schematic diagram of AQP2 maturation in renal cells.** A tentative model summarizing our current view. In the Golgi compartment, AQP2 is constitutively phosphorylated by the G-CK. Phosphorylated AQP2 is selected probably by the help of adaptor proteins recognizing phosphoserines sitting in a specific aminoacidic motif around Ser-256. AQP2-containing vesicles are probably sorted to the regulated vesicular compartment. This step would be associated with AQP2 dephosphorylation, probably accomplished by phosphatases associated with AQP2-bearing vesicles. Vasopressin stimulation controls the acute AQP2 phosphorylation by activating PKA, a signal required for AQP2 targeting to the apical plasma membrane. If AQP2 is not properly phosphorylated during its transition in the Golgi (as in E258K-AQP2 or in S256A-AQP2 expressing cells), this causes traffic of defective AQP2 to lysosomes. An essential feature in this model is the prediction that phosphorylation of AQP2 at Ser-256 is a mechanism for coupling exit from the Golgi complex and targeting to the plasma membrane.